

ECOPHYSIOLOGY

Mesothermic fishes face high fuel demands and overheating risk in warming oceans

Nicholas L. Payne^{1*}, Edward P. Snelling², Ignacio Peralta-Maraver³, David E. Cade⁴, Taylor K. Chapple⁵, Alexandra G. McInturf⁵, Yuuki Y. Watanabe⁶, David W. Sims^{7,8}, Nuno Queiroz⁹, Ivo da Costa⁹, Lara L. Sousa⁹, Jeremy A. Goldbogen⁴, Haley R. Dolton¹, Andrew L. Jackson¹

Body size and temperature set metabolic rates and the pace of life, yet our understanding of the energetics of large fishes is uncertain, especially of warm-bodied mesotherms, which can heavily influence marine food webs. We developed an approach to estimate metabolic heat production in fishes, revealing how routine energy expenditure scales with size and temperature from 1-milligram larvae up to 3-tonne megaplanktivorous sharks. We found that mesotherms use approximately four times more energy than ectotherms use and identified a scaling mismatch in which rates of heat production increase faster than heat loss as body size increases, with larger fish becoming increasingly warm bodied. This scaling imbalance creates an overheating predicament for large mesotherms, helping to explain their cooler biogeographies. Contemporary mesotherms face high fuel demands and overheating risks, which is a concern given their disproportionate demise during prior climate shifts.

A classic example of convergent evolution is seen in the physiological and biomechanical adaptations of mesothermic fishes (1). Of the thousands of extant fish species, less than 0.1% have evolved an extraordinary suite of anatomical specializations that help retain metabolic heat, with various types of mesothermy (some species warm the red muscle; others warm only the viscera or brain) having emerged at least six times among the fishes (2). Because temperature has such a dramatic impact on physiological performance (3) and water has a relatively high capacity to remove heat from submerged bodies (4), mesothermic innovations such as medial positioning of aerobic red muscle and vascular countercurrent heat exchangers help to limit heat loss to the environment, permitting faster travel speeds (5), longer migrations (6), greater power output (7), and enhanced visual acuity (8). These high-performance traits enable most mesotherms to act as top predators in wide-ranging ecosystems. Although the fast pace of a mesothermic lifestyle is associated with these ecological benefits, maintaining higher muscle temperature and faster swimming speeds both likely come with substantial challenges.

Body size, temperature, and activity level strongly influence an animal's metabolic demands, with rates of energy expenditure setting the tempo of many fundamental ecological and evolutionary processes (9). For example, metabolic rate is positively correlated with individual

and population growth rates and food requirements (9, 10) and yet may play a role in extinction risk (11). Many studies have estimated the metabolic rate of fishes by using some energy-related proxy (including mesotherms) (12), and although recent advances are providing new means of estimating metabolic rates of large fishes (13–15), there remains a relative dearth of such data (16). This knowledge gap on energetics of large fish includes uncertainty about metabolic heat flows between large fish and their environment, which are important dynamics previously invoked to explain limits to body size (17–19), extinction risk (11, 19, 20), and the evolution of endothermy in various clades (21). Accordingly, we have a poor understanding of the role of body size, temperature, and the relative cost of mesothermy in driving energy demand and heat exchange in fishes. These fundamental knowledge gaps create challenges for predicting how the world's fishes will respond to future changes in resource availability and ocean temperatures. Large-bodied and mesothermic fishes may be particularly at risk, given the high extinction rates of these species during similar environmental change in the Pleistocene (11).

We developed a method to estimate routine metabolic rate (RMR) on the basis of heat exchange of tagged fish and combined that with published respirometry data to create an RMR dataset that spans essentially the full range of body size of extant fishes (from 1-mg larvae to >3000-kg megaplanktivores) and over a large range of ocean temperatures for both ectotherms and mesotherms. By combining this new dataset with theoretical considerations of heat exchange dynamics, we addressed the question of how body size, temperature, and mesothermy set routine energy demand across the fishes. By revealing a scaling mismatch between heat production and loss, we also show a heat-imbalance problem that may especially affect large mesotherms that inhabit warm waters, which we propose helps explain their long-observed [including around the time of their emergence for some clades (22, 23)] occurrence at higher latitudes or in deeper, cooler waters (22, 24, 25)—a possibility raised half a century ago by pioneers in the field of fish energetics (26).

Estimating RMR from unsteady-state body and water temperature measurements

First, we developed a method based on biologging measurements of body temperature, water temperature, and heat exchange theory to estimate RMR of wild fishes. The theoretical basis was to use heat transfer coefficient models, which are increasingly common in studies that record temperature changes (27–29), and to model heat flow between fish and their aquatic environment. They take the form

$$\frac{dT_m(t)}{dt} = k[T_a(t) - T_m(t)] + \dot{T}O \quad (1)$$

where $T_a(t)$ and $T_m(t)$ are the empirically observed ambient water and body temperatures (degrees Celsius), respectively, at time t (seconds). Thus, $dT_m(t)/dt$ describes the “instantaneous” rate of temperature change of the body [degrees Celsius per second ($^{\circ}\text{C s}^{-1}$)] at t . The term k is the so-called whole-body heat transfer coefficient, to be estimated from a differential model and temperature data, which describes how “labile” is the body temperature relative to the temperature difference between the body and the water [the ease of body temperature change; degrees Celsius per second per degree Celsius ($^{\circ}\text{C s}^{-1} \text{ } ^{\circ}\text{C}^{-1}$)]. The product of k and $[T_a(t) - T_m(t)]$ describes the rate of temperature change of the body ($^{\circ}\text{C s}^{-1}$) due to heat flow between the body and the environment at t . The term $\dot{T}O$, also estimated from a differential model and temperature data, describes the rate of temperature change of the body ($^{\circ}\text{C s}^{-1}$) due to metabolic heat production. We propose that the rate of temperature change of the body due to metabolic heat production can now be combined with estimates of (i) how much thermal energy is needed to change the temperature of the body tissue (mass-specific heat capacity) and (ii) the corresponding amount of oxygen used during aerobic metabolism relative to the heat that is liberated (the energy

¹School of Natural Sciences, Trinity College Dublin, Dublin, Ireland. ²Department of Anatomy and Physiology, and Centre for Veterinary Wildlife Research, University of Pretoria, Onderstepoort, South Africa. ³Ecology Department and Research Unit Modeling Nature (MNat), University of Granada, Granada, Spain. ⁴Hopkins Marine Station, Stanford University, Monterey, CA, USA. ⁵Coastal Oregon Marine Experiment Station, Oregon State University, Newport, OR, USA. ⁶Research Center for Integrative Evolutionary Science, The Graduate University for Advanced Studies, Sokendai, Hayama, Japan. ⁷Marine Biological Association, The Laboratory, Plymouth, UK. ⁸Ocean and Earth Science, National Oceanography Centre Southampton, University of Southampton, Southampton, UK. ⁹CIBIO, Centro de Investigação em Biodiversidade e Recursos Genéticos, Universidade do Porto, Vairão, Portugal. *Corresponding author. Email: paynen@tcd.ie

equivalence of oxygen) to calculate whole-body oxygen consumption rate (denoted as RMR, in milligrams of O_2 per second) as

$$\text{RMR} = Q_{\text{ox}} \dot{T} O C M = 0.245 \dot{T} O M \quad (2)$$

Where Q_{ox} is the energy equivalence of oxygen [$0.070 \text{ mg } O_2 \text{ J}^{-1}$, assuming a respiratory quotient of 0.80 (30)], C is the average mass-specific heat capacity of tissue [$3.5 \text{ J } C^{-1} \text{ g}^{-1}$ (31)], and M is fish mass in grams.

A lack of data from very large fishes prompted us to tag seven free-swimming basking sharks (*Cetorhinus maximus*), of ~800 to 3500 kg body mass, with body and ambient temperature sensors [supplementary materials (SM), materials and methods] and fit Eq. 1 to the resulting T_a and T_m data to (simultaneously) estimate $\dot{T}O$ and k for those seven sharks (fig. S1). We then extracted data from previous published studies, using similar tagging procedures, that also report model outputs of $\dot{T}O$. This yielded 43 data points from 10 species, including both ectotherms and mesotherms smaller than 10 kg and larger than 1500 kg (SM materials and methods and data S1). We then used Eq. 2 to estimate RMR for these 43 data points.

A consistent energetic cost of increasing body size, temperature, and mesothermy

We combined the RMR data estimated with our heat-exchange method with estimates of RMR calculated with the more traditional method of quantifying oxygen consumption rate by means of respirometry (data S1). To do this, we conducted a literature search (SM materials and methods), which returned 443 measurements of RMR from 137 species and a mass range of ~1 mg to 126 kg and temperature range of 0° to 35°C . We analyzed the combined RMR data (from our heat exchange and respirometry methods) by

$$\text{RMR}(S) = e^{\gamma(S)} e^{\beta T_m} M^\alpha \quad (3)$$

with a Bayesian mixed-effects model regression (SM materials and methods) to describe how RMR varies with body mass M (α), body temperature T_m (β), and thermal strategy (S ; whether the fish is a mesotherm or ectotherm), with the intercept as γ . An additional fixed effect of method (heat-exchange versus respirometry) was not supported by model selection, nor was inclusion of a mass \times method interaction term. Together, these results indicate that estimating RMR by means of temperature biologging provides a reliable proxy for routine oxygen consumption in large fishes, and that metabolic scaling relationships established for smaller-bodied fishes by using respirometry extend to the largest extant fishes, including ectothermic whale sharks and mesothermic basking sharks (32). Our results were similar whether we used measured body temperature at the location of the probe or the estimated core body temperature of tagged fish to estimate RMR (SM materials and methods). The final simplified model describing RMR (in milligrams of O_2 per hour) was

$$\text{RMR} = e^\gamma e^{0.093 T_m} M^{0.827} \quad (4)$$

where γ is 3.99 for mesotherms and 2.66 for ectotherms, and body mass M is in kilograms. Accordingly, after accounting for variation in body temperature, fish RMR is 3.78-fold higher for mesotherms than for ectotherms, and this disparity is consistent across the full body size range

of fishes (Fig. 1B). When controlling for body mass and thermal strategy, the influence of body temperature ($\beta = 0.093$) is equivalent to a 2.53-fold increase in fish RMR for a 10°C increase in T_m ($e^{10 \times 0.093}$). The average coefficient of determination (R^2) derived from the model's posterior parameter distribution was 0.97. All resulting model outputs are presented in tables S1 and S2.

Our results indicate that the fast pace of a mesothermic lifestyle comes with major, and relatively persistent, energy cost regardless of body size. The higher body temperatures of mesotherms cannot explain the difference because the ~3.8-fold elevation in energy expenditure exists after controlling for body temperature. Mesothermic fishes are famously fast, with best estimates suggesting 1.6 to 2.7 times faster routine cruising speeds compared with that of similarly sized ectothermic counterparts (5, 6). These high metabolic rates must be largely met by increased food consumption, and when temperature varies, the mesotherms experience large variation in the magnitude of energy requirements. For example, in Fig. 2A we show how RMR will vary for fish of different body sizes when body temperature T_m ranges from 20° to 25°C . This likely comes with certain physiological or behavioral consequences and may further make them sensitive to changing biotic or abiotic conditions (11). Another consequence is a high rate of heat production, which theoretically comes with its own implications.

Larger fish become increasingly warm bodied

Combining Eqs. 2 and 4 allows for the estimation of the rate of temperature change of the body ($^\circ\text{C } s^{-1}$) due to metabolic heat production, $\dot{T}O$, for a fish of any body mass, T_m , and thermal strategy S (SM materials and methods). On the basis of Newtonian cooling and Euclidean geometry, we would expect k ($^\circ\text{C } s^{-1} \text{ } ^\circ\text{C}^{-1}$) to vary $\sim M^{-0.33}$, but a compilation of 103 in vivo measurements of k from 19 species [excluding the two megaplanktivore species—basking sharks and whale sharks—which have unusually high k (SM materials and methods)] reveals a much steeper negative exponent, with

$$k(^\circ\text{C } s^{-1} \text{ } ^\circ\text{C}^{-1}) = 0.00174 M^{-0.632} \quad (5)$$

The steep negative exponent of approximately -0.63 suggests that larger fishes are less thermally labile even after accounting for their presumably smaller surface-area-to-volume ratios. Combining this

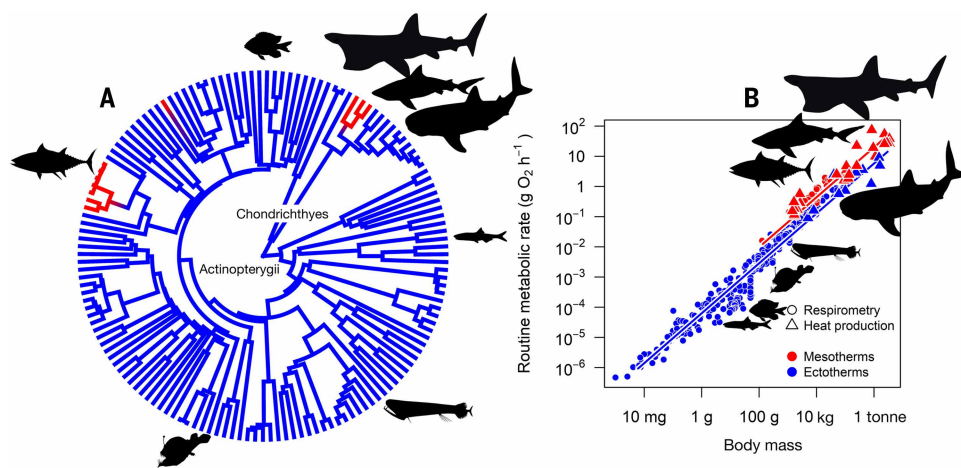


Fig. 1. A persistently higher energetic cost to fuel mesothermy in fishes. (A) The phylogeny used in the regression of body mass, body temperature, and thermal strategy (red, mesotherms; blue, ectotherms) on (B) fish RMR (plotted data are temperature corrected). Triangles indicate RMR estimated with our heat production method, with all other data derived from respirometry. Fitted equations are $\text{RMR} = e^{3.988} e^{0.093 T_m} M^{0.827}$ for mesotherms and $\text{RMR} = e^{2.658} e^{0.093 T_m} M^{0.827}$, where M is body mass (kilograms) and T_m is body temperature ($^\circ\text{C}$). The average R^2 derived from the model's posterior parameter distribution was 0.97.

empirically derived scaling of the ease of heat loss with that of heat generation ($RMR \sim M^{0.83}$) suggests that larger fish generate heat faster than they lose it, and we can estimate the effect of the surplus heat on body temperature by referring back to Eq. 1, revealing that

$$T_m - T_a = \varepsilon M^{0.459} e^{0.093 T_m} \quad (6)$$

where the scaling coefficient ε is 0.0305 for mesotherms and 0.0081 for ectotherms. Equation 6 shows that T_m will be increasingly elevated above T_a as M increases and as T_m increases, especially for mesotherms (Fig. 2B). This equation describes empirically the gigantothermy phenomenon in fishes and how it varies depending on thermal strategy. Previous studies on mammals (33), sea turtles (4), and theropods (21) have invoked similar ideas on scaling mismatches of heat generation and thermal conductance in attempts to understand emergence of phenomena such as animals tending to be smaller toward the equator (Bergmann's Rule) (18) and why endothermy evolved with miniaturization in vertebrate lineages (21). The gigantothermy exponent for fishes (0.46) is similar to that predicted (0.42) for sea turtles (4) and higher than that of theropod dinosaurs (0.25) (21), which is perhaps surprising

given that the thermal conductivity of water is approximately 25-fold greater than that of air (34) and that gas- and heat-exchange across the gills are thought to be closely coupled in fish (35). Nevertheless, the modest scaling coefficient (0.0081) for ectotherms produces notable albeit much smaller absolute T_m elevations above T_a compared with those of mesotherms (Fig. 2B), showcasing the relative warm-bodiedness for which mesotherms are renowned. Curiously, the similar scaling of k between ectotherms and mesotherms (28) suggests that the elevated body temperatures of mesotherms arise not because of large differences in whole-body thermal conductance (as might be expected given that heat exchangers are assumed to reduce convective heat loss) but primarily because of much higher rates of heat production, which is itself increased by elevated body temperature (with a $Q_{10} \sim 2.5$, where Q_{10} is the increase in rate of a chemical reaction for each 10°C increase in temperature). Accordingly, the thermal physiology of mesotherms might best be considered singular in their production of heat through high metabolic rates, not just its retention through anatomical specializations. Such a perspective could also help circumvent some of the debate on how best to define and classify mesotherms given the variety of anatomical structures they exhibit for retaining heat.

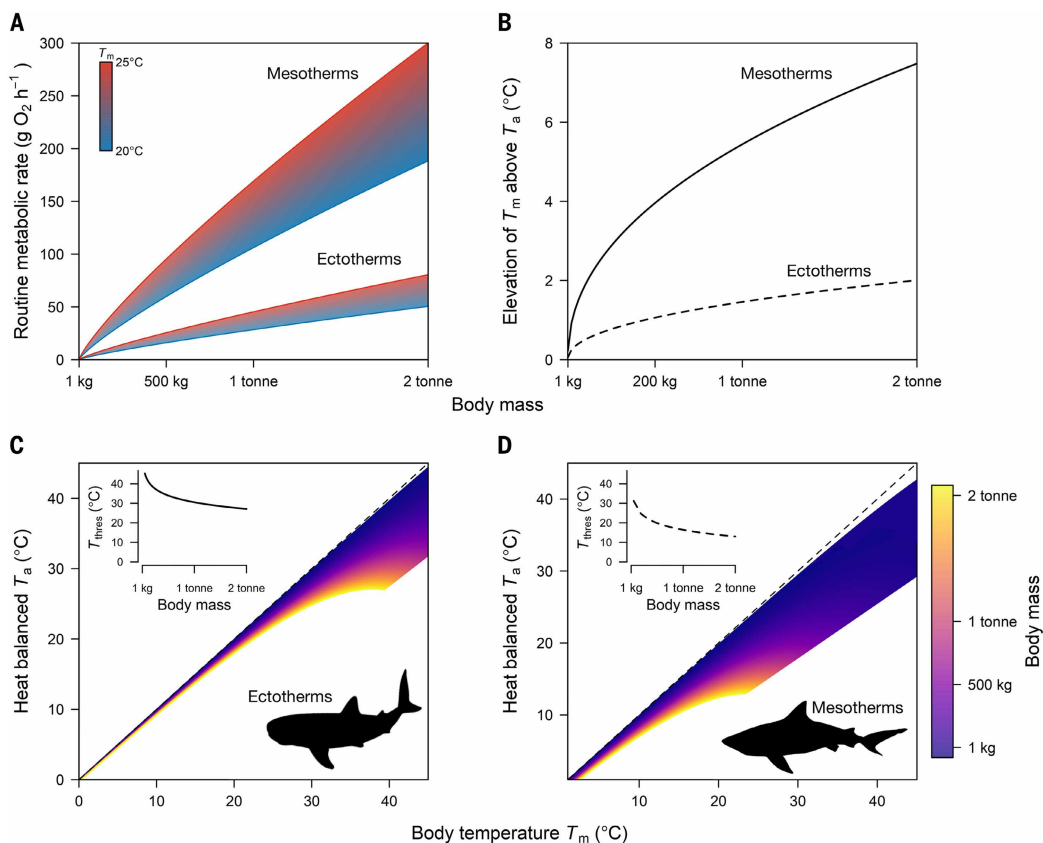


Fig. 2. Scaling of energy demand and heat balance thresholds in large-bodied fishes. (A) RMR is ~3.8-fold higher for mesotherms than for ectotherms and fluctuates widely for the mesotherms as body temperature varies. Plotted are estimates of RMR experienced by fish between 20° and 25°C body temperature T_m , with RMR estimated on the basis of Eq. 4 and the predictFishRMR package (36). (B) The empirically derived gigantothermy phenomenon in fish shows how bigger fish—particularly mesotherms—have elevated body temperature owing to a scaling mismatch between heat production and loss. Shown is the estimated elevation of body temperature T_m above water temperature T_a when T_m is 20°C. (C and D) Main axes show estimated T_m for fish of various body mass when in heat balance while swimming in various T_a . The curved relationships between T_a and T_m under heat balance produce upper thresholds (T_{thres}) of T_a beyond which fish of certain mass cannot balance heat production and loss unless they engage physiological or behavioral adjustments. (Inset) These theoretical heat balance thresholds T_{thres} . Larger fish have lower T_{thres} , especially mesotherms, given higher rates of heat production. The dashed line indicates the identity line.

A general model of fish RMR during heat balance

Previous equations can be rearranged to estimate T_m for any T_a when a fish is in heat balance with its environment—that is, under steady-state conditions, when the rate of heat production is equal to that of heat loss so that the fish is neither heating nor cooling (mathematical steps are provided in the SM materials and methods). This produces a general model for estimating RMR of a fish of any size and thermal strategy if body temperature is unknown but water temperature is known, and assuming the fish is in heat balance [a worked example is available in (36)]. This model also shows how the higher T_m elevation of mesotherms accentuates the disparity of their energy demands over ectotherms, particularly large ones. For example, a 500-kg mesotherm has a ~5.1-fold higher RMR than the same size ectotherm if they are both in 20°C water, compared with a ~3.8-fold difference if they both have the same T_m .

Overheating risk and thermal niches of large and mesothermic fishes

Empirical solutions to our heat balance equation (SM materials and methods, eq. S8) show that as fishes encounter warmer water temperatures, their body temperature increases at a faster rate, particularly for larger fish and mesotherms (Fig. 2, C and D). These trends are a manifestation

of the scaling mismatch between heat production and ease of heat loss and compounded by the much higher RMR and thus heat generation of mesotherms. The curved form of the heat balance model also reveals upper thresholds of T_a above which there appear no empirical solutions for fishes to remain in heat balance if they follow the observed scaling patterns (Fig. 2, C and D, insets). We call these maximum T_a heat balance thresholds T_{thres} . For example, our model predicts that a 2-tonne ectotherm (such as a whale shark) has $T_{\text{thres}} \sim 27^\circ\text{C}$, but T_{thres} is as low as 20° and 17°C for a 500-kg and 1-tonne mesotherm, respectively (Fig. 2, C and D, and fig. S6). Above those model-predicted T_a heat balance thresholds, fish will continue to heat unless they reduce their rate of heat production (lower RMR by swimming slower), increase their cooling rate, or both. Consequently, our models would predict that the strong influence of body size and thermal strategy on heat-balance thresholds T_{thres} should impose a biogeographic pattern of a decline in body size toward the equator and a tendency for mesotherms (especially large ones) to prefer cooler latitudes to avoid overheating. Both patterns have been observed for decades (17, 18, 22, 24, 37) but are traditionally explained by very different physiological (38, 39) or ecological (24, 25) processes.

The overheating challenge may help explain old patterns (for example, why mesothermy in fishes seemed to emerge during a period of ocean cooling, and extension of ancestral mesotherms toward higher latitudes, at least for the Lamnidae) (22, 23) and predict new ones. Our model-predicted T_{thres} values are broadly consistent with the observed differences in the distributions of large ectotherms versus mesotherms and how their peak occurrences vary between seasons through latitudinal migrations. To illustrate this, in Fig. 3 we show current and future global sea surface temperatures (modeled with Bio-ORACLE, Lt. max and min) (40, 41) for the average temperature of the coolest (winter) and warmest (summer) months of each hemisphere in terms of the corresponding RMR estimated from the best fits of our model, and with white areas indicating sea surface temperatures exceeding estimated T_{thres} for two example fishes. Avoiding T_{thres} would predict large fishes—especially mesotherms—to be restricted to higher latitudes or greater depths,

increasingly during the summer months and under future warming scenarios (Fig. 3 and fig. S5).

Can big fish avoid overheating by modulating thermal conductance?

Our results on overheating thresholds T_{thres} are based on the average observed relationships between rates of heat production and ease of heat loss, yet some fishes—particularly several tuna species—can substantially vary thermal conductance, which could help reduce overheating risk in warm water (sensitivity analyses are available in SM materials and methods and fig. S6). For example, Atlantic bluefin tuna *T. thynnus* dramatically increase k as they encounter waters at approximately the temperature that our model predicts as an overheating threshold (fig. S7) (42). There is less evidence of thermal conductance plasticity in other mesothermic or ectothermic fishes, although the tagged basking sharks and whale sharks had unusually high thermal conductance for their size (fig. S4), possibly reflecting some acute or evolutionary link between gigantism, planktivory, and a filter-feeding lifestyle [similarly sized nonfilter-feeding great white sharks *Carcharodon carcharias*, on the other hand, exhibit k that is in line with all other data (fig. S4)]. Basking sharks have many mesothermic features (32), including elevated RMR (Fig. 1), but lack red muscle heat-exchangers (43), an unusual vascular configuration that potentially facilitates mesothermy and gigantism yet avoids overheating when they periodically transit warm surface temperatures (44). Many large fish species also exhibit regular excursions to deeper ocean layers (45), a behavior often interpreted as thermoregulation (46). Evidently, there potentially are both physiological and behavioral solutions that enable large fishes to inhabit temperatures exceeding their theoretical T_{thres} —which they often do (42, 47, 48). Nevertheless, even tunas with the now-famous physiological thermoregulatory capabilities (35, 49, 50) may not be able to completely bypass overheating challenges: Although bluefin tuna can increase rates of heat loss in waters exceeding their theoretical T_{thres} (fig. S7), it also seems necessary for them to dive to cooler depths at the same time (42); they have high mortality rates if restricted to warm surface waters (51). Accordingly, our estimates of heat balance thresholds

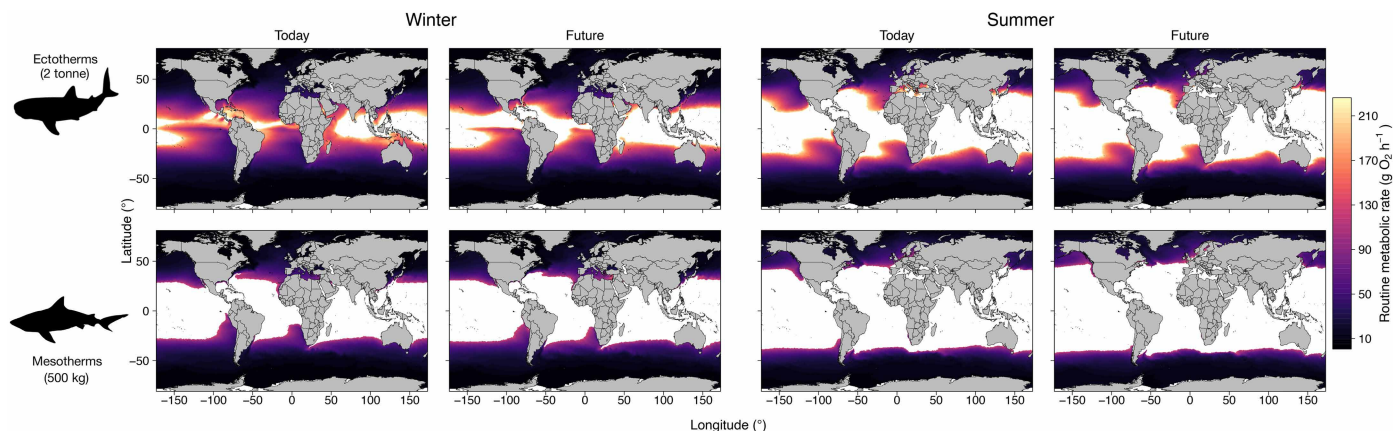


Fig. 3. Energy landscape and theoretical heat balance thresholds for contemporary and future large-bodied fishes. RMR increases with water temperature and body size and is higher for mesothermic than for ectothermic fishes. In all maps, RMR is estimated for current and future sea surface temperature scenarios (40, 41) for a model 2-tonne ectotherm and 500-kg mesotherm by using Eqs. 4 and S8, with white regions indicating surface temperatures that exceed the theoretical thresholds T_{thres} beyond which those fish cannot balance heat production and loss unless engaging behavioral (for example, diving to cooler depths as seen in salmon sharks) (25) or physiological mechanisms (for example, swimming more slowly or altering blood circulation patterns, as seen in bluefin tuna) (42). These heat-balance dynamics could help explain why large fishes migrate seasonally (winter, left, versus summer, right) and why contemporary mesotherms are distributed toward higher latitudes than those of ectotherms (top versus bottom) and could help predict range shifts for large fishes under future ocean warming (“Today” versus “Future” sea surface temperature scenarios). Scenario SSP4-6.0 was used to generate future warming scenarios (2080–2100), and all plots show the average temperature of the coolest (winter) and warmest (summer) months during a given decade. “Today” conditions have been defined here as baseline sea surface temperature for the decade between 2010 and 2020.

should not be considered rigid environmental temperature limits of a species but rather thermal boundaries that, when crossed, demand physiological or behavioral adjustment. Better understanding the capabilities and associated costs of such adjustment across species could help predict which fishes will be more reliant on shifting to cooler latitudes [for example, (52, 53)] or depths (42) in future oceans and which can largely buffer overheating risk by modulating heat flow. A more challenging task might be predicting the role of evolutionary adaptation in coping with thermal challenges in future oceans; our results suggesting current (fig. S4) and past (54) ocean giants could be a fruitful focus for this pursuit, given apparent and presumed (respectively) unusually high thermal conductance supporting gigantism.

Challenges ahead for contemporary mesothermic species

The fast pace of mesothermy clearly confers benefits, but our results highlight several trade-offs that are especially relevant today given the ongoing changes to our oceans. Mesotherms require around 3.8 times more energy than required by ectotherms, and this disparity is even greater if they are inhabiting the same water temperature (because according to our models, the mesotherm will operate at a higher T_m). Greater resource demands of maintaining warmer bodies have been implicated in setting size limits (19, 20) and extinction rates (11) for a range of extant and extinct vertebrate clades, including the enigmatic and presumed mesothermic megatooth shark *Otodus megalodon* (54, 55)—a challenge exacerbated for mesotherms living in the Anthropocene because many of their prey species are heavily extracted for human consumption (56). Mesotherms, and to a lesser extent large ectotherms, face the added heat-balance problem, which seemingly precludes them from warm waters or necessitates physiological or behavioral adjustments to break away from our observed scaling patterns. Taken together, large fishes, particularly mesotherms, likely face increased resource demands and further displacement toward the poles given the strong influence of temperature on their physiological and physical dynamics. Many mesothermic fishes are additionally under severe pressure from overfishing and already classified as endangered or vulnerable, which is cause for concern that today's mesotherms may be at risk of similarly disproportionate extinction rates as those of their warm-bodied Pleistocene counterparts (11).

REFERENCES AND NOTES

- J. M. Donley, C. A. Sepulveda, P. Konstantinidis, S. Gemballa, R. E. Shadwick, *Nature* **429**, 61–65 (2004).
- L. J. Legendre, D. Davesne, *Philos. Trans. R. Soc. Lond. B Biol. Sci.* **375**, 20190136 (2020).
- A. I. Dell, S. Pawar, V. M. Savage, *Proc. Natl. Acad. Sci. U.S.A.* **108**, 10591–10596 (2011).
- K. Sato, *J. Exp. Biol.* **217**, 3607–3614 (2014).
- L. Harding *et al.*, *Funct. Ecol.* **35**, 1951–1959 (2021).
- Y. Y. Watanabe, K. J. Goldman, J. E. Caselle, D. D. Chapman, Y. P. Papastamatiou, *Proc. Natl. Acad. Sci. U.S.A.* **112**, 6104–6109 (2015).
- D. Bernal, J. M. Donley, R. E. Shadwick, D. A. Syme, *Nature* **437**, 1349–1352 (2005).
- K. A. Fritsches, R. W. Brill, E. J. Warrant, *Curr. Biol.* **15**, 55–58 (2005).
- J. H. Brown, J. F. Gillooly, A. P. Allen, V. M. Savage, G. B. West, *Ecology* **85**, 1771–1789 (2004).
- S. Gravel, J. S. Bigman, S. A. Pardo, S. Wong, N. K. Dulvy, *Fish Fish.* **25**, 349–361 (2024).
- C. Pimiento *et al.*, *Nat. Ecol. Evol.* **1**, 1100–1106 (2017).
- J. M. Blank, C. J. Farwell, J. M. Morrisette, R. J. Schallert, B. A. Block, *Physiol. Biochem. Zool.* **80**, 167–177 (2007).
- C. N. Trueman *et al.*, *Nat. Commun.* **14**, 7379 (2023).
- M.-T. Chung, C. N. Trueman, J. A. Godiksen, M. E. Holmstrup, P. Grønkvær, *Commun. Biol.* **2**, 24 (2019).
- K. O. Lear *et al.*, *J. Exp. Biol.* **220**, 397–407 (2017).
- N. L. Payne *et al.*, *Methods Ecol. Evol.* **6**, 668–677 (2015).
- D. Atkinson, *Adv. Ecol. Res.* **25**, 1–58 (1994).
- C. Bergmann, *Über die Verhältnisse der Wärmeökonomie der Thiere zu ihrer Grösse* (Vandenhoeck und Ruprecht, 1848).
- B. K. McNab, *Proc. Natl. Acad. Sci. U.S.A.* **106**, 12184–12188 (2009).
- B. K. McNab, *J. Zool.* **199**, 1–29 (1983).
- E. L. Rezende, L. D. Bacigalupe, R. F. Nespolo, F. Bozinovic, *Sci. Adv.* **6**, eaaw4486 (2020).
- K. A. Dickson, J. B. Graham, *Physiol. Biochem. Zool.* **77**, 998–1018 (2004).
- R. W. Purdy, in *Great White Sharks: The Biology of Carcharodon Carcharias*, A. P. Klimley, D. G. Ainley, Eds. (Academic Press, 1996), pp. 67–78.
- J. M. Grady *et al.*, *Science* **363**, eaat4220 (2019).
- K. C. Weng *et al.*, *Science* **310**, 104–106 (2005).
- R. A. Barkley, W. H. Neill, R. Gooding, *Fish Bull.* **76**, 653–662 (1978).
- H. Malte, C. Larsen, M. Musyl, R. Brill, *J. Exp. Biol.* **210**, 2618–2626 (2007).
- I. Nakamura, R. Matsumoto, K. Sato, *J. Exp. Biol.* **223**, jeb210286 (2020).
- Y. Y. Watanabe, I. Nakamura, W.-C. Chiang, *Mar. Biol.* **168**, 161 (2021).
- K. Schmidt-Nielsen, *Animal Physiology: Adaptation and Environment* (Cambridge Univ. press, 1997).
- K. Giering, I. Lamprecht, O. Minet, *Laser-Tissue Interaction and Tissue Optics* **2624**, 188–197 (1996).
- H. Dolton *et al.*, *Endanger. Species Res.* **51**, 227–232 (2023).
- B. K. McNab, *Am. Nat.* **112**, 1–21 (1978).
- P. Dejours, *Principles of Comparative Respiratory Physiology* (Elsevier, ed. 2, 1981).
- R. W. Brill, H. Dewar, J. B. Graham, *Environ. Biol. Fishes* **40**, 109–124 (1994).
- A. L. Jackson, predictFishRMR. GitHub repository (2025); <https://github.com/AndrewLJackson/predictFishRMR>.
- R. J. Walters, M. Hassall, *Am. Nat.* **167**, 510–523 (2006).
- W. C. E. P. Verberk *et al.*, *Biol. Rev. Camb. Philos. Soc.* **96**, 247–268 (2021).
- D. Pauly, *Sci. Adv.* **7**, eabc6050 (2021).
- J. Assis *et al.*, *Glob. Ecol. Biogeogr.* **33**, e13813 (2024).
- L. Tyberghein *et al.*, *Glob. Ecol. Biogeogr.* **21**, 272–281 (2012).
- S. L. Teo *et al.*, *Mar. Biol.* **151**, 1–18 (2007).
- C. A. Klöcker *et al.*, *J. Fish Biol.* **jfb.70052** (2025).
- C. D. Braun, G. B. Skomal, S. R. Thorrold, *Front. Mar. Sci.* **5**, 25 (2018).
- S. Andrzejczek *et al.*, *Sci. Adv.* **8**, eab01754 (2022).
- M. Thums, M. Meekan, J. Stevens, S. Wilson, J. Polovina, *J. R. Soc. Interface* **10**, 20120477 (2013).
- K. C. Weng *et al.*, *Mar. Biol.* **152**, 877–894 (2007).
- J. J. Vaudo, M. E. Byrne, B. M. Wetherbee, G. M. Harvey, M. S. Shivji, *J. Appl. Ecol.* **54**, 1765–1775 (2017).
- A. E. Dizon, R. W. Brill, *Am. Zool.* **19**, 249–265 (1979).
- H. Dewar, J. Graham, R. Brill, *J. Exp. Biol.* **192**, 33–44 (1994).
- B. A. Block *et al.*, *Nature* **434**, 1121–1127 (2005).
- J. J. Dale *et al.*, *Divers. Distrib.* **28**, 2020–2034 (2022).
- G. E. McNicholas *et al.*, *Divers. Distrib.* **30**, e13865 (2024).
- M. L. Griffiths *et al.*, *Proc. Natl. Acad. Sci. U.S.A.* **120**, e2218153120 (2023).
- C. Pimiento *et al.*, *J. Biogeogr.* **43**, 1645–1655 (2016).
- D. Pauly, V. Christensen, J. Dalsgaard, R. Froese, F. Torres Jr., *Science* **279**, 860–863 (1998).

ACKNOWLEDGMENTS

We thank three anonymous reviewers for constructive feedback on earlier drafts of the work. **Funding:** Funding for this project was provided by Research Ireland (18/SIRG/5549), Marine Institute (PD PDOC/21/04/01), Irish Research Council (IRCLA/2017/186), Future Legend Films, Oregon State University, National Geographic and Human Frontier Science Program (HFSP-RGPO010/2020), Japan Society for the Promotion of Science (22K21355 and 23K27251), and Fundação para a Ciência e a Tecnologia (FCT; PTDC/BMA/3536/2021 and CEECIND/02857/2018). **Author contributions:** Conceptualization: N.L.P., E.P.S., I.P.-M., A.L.J. Investigation: All authors. Methodology: N.L.P., E.P.S., I.P.-M., A.L.J. Formal analyses: N.L.P., E.P.S., I.P.-M., A.L.J. Funding acquisition: N.L.P., H.R.D., T.K.C., A.G.M., J.A.G. Writing - original draft: N.L.P. Writing - reviewing & editing: All authors. Project administration: N.L.P. **Competing interests:** The authors declare no competing interests. **Data and materials availability:** All data are available in the manuscript or supplementary materials, and our code is available at <https://github.com/AndrewLJackson/predictFishRMR>. **License information:** Copyright © 2026 the authors, some rights reserved; exclusive licensee American Association for the Advancement of Science. No claim to original US government works. <https://www.science.org/about/science-licenses-journal-article-reuse>. This research was funded in whole or in part by Research Ireland (18/SIRG/5549) and Irish Research Council (IRCLA/2017/186), cOAlition S organizations. The author will make the Author Accepted Manuscript (AAM) version available under a CC BY public copyright license.

SUPPLEMENTARY MATERIALS

[science.org/doi/10.1126/science.adt2981](https://doi.org/10.1126/science.adt2981)
Materials and Methods; Figs. S1 to S7; Tables S1 and S2; References (57–64); MDAR Reproducibility Checklist; Data S1; Code S1

Submitted 25 September 2024; resubmitted 6 November 2025; accepted 19 February 2026

[10.1126/science.adt2981](https://doi.org/10.1126/science.adt2981)



Mesothermic fishes face high fuel demands and overheating risk in warming oceans

Nicholas L. Payne, Edward P. Snelling, Ignacio Peralta-Maraver, David E. Cade, Taylor K. Chapple, Alexandra G. McInturf, Yuuki Y. Watanabe, David W. Sims, Nuno Queiroz, Ivo da Costa, Lara L. Sousa, Jeremy A. Goldbogen, Haley R. Dolton, and Andrew L. Jackson

Science **392** (6795), . DOI: 10.1126/science.adt2981

Editor's summary

Body size and metabolic rate are intertwined, a factor that is especially important to understand with regard to animals that live in aquatic environments, where heat loss is related to water temperature. Payne *et al.* developed a method to estimate routine metabolic rate based on measures from tagged fish, and combined the estimates with published respirometry rates to create a dataset spanning the entire body size range of extant fishes. Using these data, the authors found a scaling imbalance between heat production and loss that affects especially large, mesothermic fishes in warm waters. This imbalance both explains the distribution of these fish in cooler waters and suggests a special sensitivity to warming waters. —Sacha Vignieri

View the article online

<https://www.science.org/doi/10.1126/science.adt2981>

Permissions

<https://www.science.org/help/reprints-and-permissions>

Use of this article is subject to the [Terms of service](#)

Science (ISSN 1095-9203) is published by the American Association for the Advancement of Science. 1200 New York Avenue NW, Washington, DC 20005. The title *Science* is a registered trademark of AAAS.

Copyright © 2026 The Authors, some rights reserved; exclusive licensee American Association for the Advancement of Science. No claim to original U.S. Government Works